Inorg. Chem. **2006**, *45*, 2562–2567

$Co_3(RL)_2(hfac)_6$ Ladder Complex of 5-[4-(*N*-*tert*-Butyl-*N*-aminoxyl)phenyl]pyrimidine

Lora M. Field,[†] M. Carmen Morón,[‡] Paul M. Lahti,*[,†] Fernando Palacio,[‡] Armando Paduan-Filho,[§] and Nei F. Oliveira Jr.[§]

Department of Chemistry, University of Massachusetts, Amherst, Massachusetts 01003, Instituto de Ciencia de Materiales de Aragón, CSIC, Universidad de Zaragoza, 50009 Zaragoza, Spain, and Instituto de Fisica, Universidade de São Paulo, São Paulo, Brazil

Received October 31, 2005

5-[4-(*N*-*tert*-butyl-*N*-aminoxyl)phenyl]pyridimine (4NITPhPyrim = RL) forms a 1-D ladder polymer complex with $Co(hfac)_2$ of stoichiometry $Co_3(RL)_2(hfac)_6$, having antiparallel $[Co^{II}RL]_n$ linear chains (rails) that are cross-linked by Pyrim–$Co(hfac)_2$–Pyrim rungs. The magnetic behavior above 100 K is consistent with contributions from one high-spin Co^{II} ion (the cross-link, $S = {}^3/_2$) plus two Co–ON units with strongly antiferromagnetic (AFM) metal–radical exchange (each $S = 1$). The χT data show an AFM downturn as the temperature drops. Assuming weak exchange along chain portions of the polymer due to poor spin polarization across the phenyl–pyrimidine bond in RL, a linear three-spin ($S = 1$, $^3/_2$, and 1) fit to the $T > 18$ K data yields an AFM cross-linker (rung) effective exchange of $J_{CL}/k = (-)5.3\ K = (-)3.7\ cm^{-1}$. Superexchange ($\sigma$-orbital overlap) is a likely mechanism for the effective AFM exchange between CoON and Co spin sites in the three-spin groupings.

Introduction

Hybrid coordination complexes made with paramagnetic ions and radical ligands are of much interest[1] to find combinations that yield higher dimensionality coordination and to investigate exchange behaviors between unpaired spins on the organic radical and inorganic ion portions of the structure. We previously reported[2] cyclic $M_2(RL)_2(hfac)_4$ type complexes **1** (Chart 1) of $Mn(hfac)_2$ and $Cu(hfac)_2$ with radical ligand 5-[4-(*N*-*tert*-butyl-*N*-aminoxyl)phenyl]pyridimine (4NITPhPyrim = RL). These exhibit strong antiferromagnetic (AFM) and ferromagnetic (FM) M−ON exchange coupling for Mn^{II} and Cu^{II}, respectively, with weak AFM exchange between M−ON units. While neither Mn^{II} nor Cu^{II} forms extended chain or network complexes with 4NITPhPyrim, $Co(hfac)_2$ forms a 1-D ladder polymer. Here we report the structural and magnetic characterization of this complex, **2** (Chart 1).

Results

Layered solutions of 4NITPhPyrim = RL[2,3] and $Co(hfac)_2 \cdot xH_2O$ yield **2** as a dark-green solid with an elemental analysis consistent with stoichiometry $Co_3(RL)_2(hfac)_6$. Excess $Co(hfac)_2 \cdot xH_2O$ is required because use of excess radical yields complex **3** (Chart 1) with stoichiometry $Co(RL)_2(hfac)_2$.[4] No cyclic $Co_2(RL)_2(hfac)_4$ analogous to **1** was obtained under any conditions attempted. Single-crystal X-ray diffraction analysis of **2** at room temperature yields the structure shown in Figure 1. Table 1 lists selected crystallographic and structural results. Full details in

* To whom correspondence should be addressed. E-mail: lahti@chem.umass.edu.
[†] University of Massachusetts.
[‡] Universidad de Zaragoza.
[§] Universidade de São Paulo.

(1) (a) Kahn, O. *Molecular Magnetism*; VCH: New York, 1993. (b) Iwamura, H.; Inoue, K.; Hayamizu, T. *Pure Appl. Chem.* **1996**, *68*, 243. (c) Caneschi, A.; Gatteschi, D.; Sessoli, R.; Rey, P. *Acc. Chem. Res.* **1989**, *22*, 392. (d) Caneschi, A.; Gatteschi, D.; Sessoli, R. In *Magnetic Molecular Materials*; Gatteschi, D., Kahn, O., Miller, J. S., Palacio, F., Eds.; Kluwer: Dordrecht, The Netherlands, 1991; p 215. (e) Gatteschi, D.; Rey, P. In *Magnetic Properties of Organic Materials*; Lahti, P. M., Ed.; Marcel Dekker: New York, 1999. (f) Caneschi A.; Gatteschi, D.; Rey, P. In *Progress in Inorganic Chemistry*; Lippard, S. J., Ed.; Wiley: New York, 1991; Vol. 39, p 331. (g) Ouahab, L. *Coord. Chem. Rev.* **1998**, *178*−*180*, 1501. (h) Hicks, R. G. *Aust. J. Chem.* **2001**, *54*, 597. (i) Lemaire, M. T. *Pure Appl. Chem.* **2004**, *76*, 277.
(2) Field, L. M.; Lahti, P. M.; Palacio, F.; Paduan-Filho, A. *J. Am. Chem. Soc.* **2003**, *125*, 10110.
(3) Field, L. M.; Lahti, P. M. *Polyhedron* **2005**, *24*, 2639.
(4) Field, L. M. The Synthesis and Magnetism of Nitroxide Radicals and Their Metal Complexes. Ph.D. Dissertation, University of Massachusetts, Amherst, MA, 2003.

10.1021/ic051884w CCC: $33.50
Published on Web 02/11/2006

Chart 1

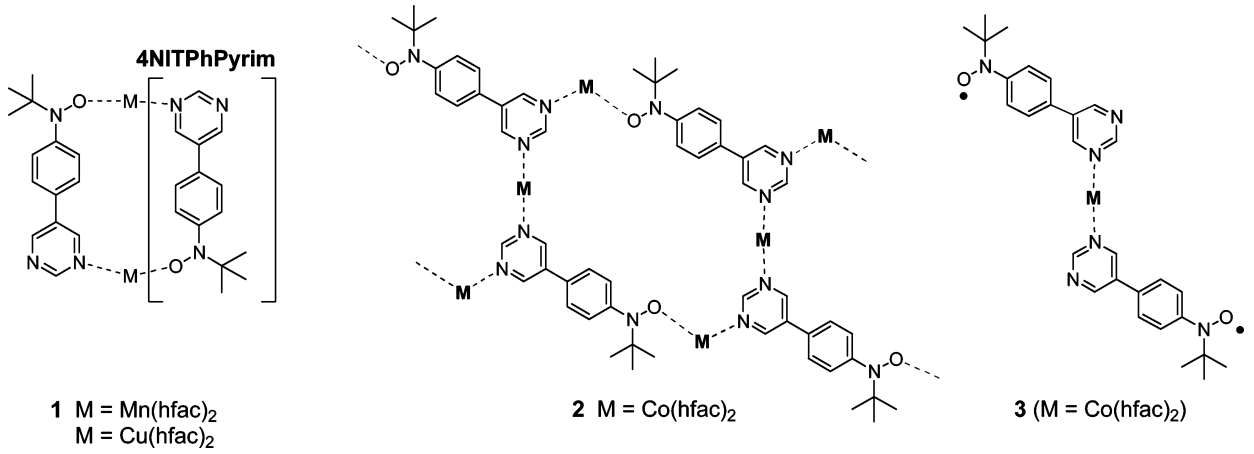

CIF format are available as Supporting Information and were also deposited at the Cambridge Crystallographic Databank.

Magnetic susceptibility (χ) versus temperature measurements on a polycrystalline sample of **2** yielded the χT vs T and $1/\chi$ vs T data that are shown in Figure 2. Magnetization versus field studies on powdered samples yielded the M_{molar} vs H data shown in Figure 3. Interpretive analyses of the data are given in the Discussion section.

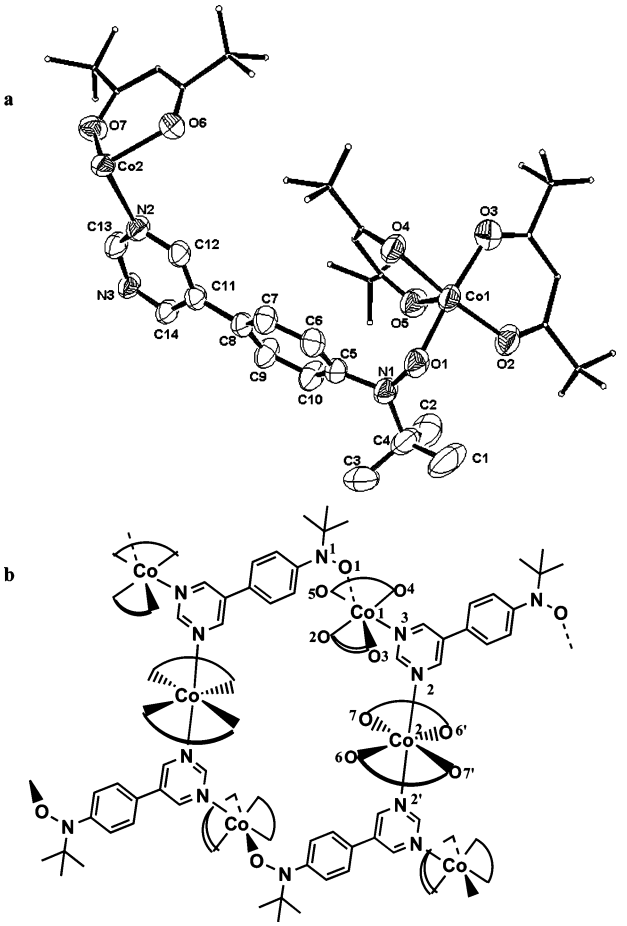

Figure 1. (a) ORTEP representation of **2** at room temperature, using 50% probability ellipsoids. (b) Schematic representation of **2** with atom numbering from the ORTEP diagram. Hydrogen and fluorine atoms are omitted for ease of viewing.

Table 1. Crystallographic Analysis Data for Complex **2**

chemical formula	$C_{58}H_{38}Co_3F_{26}N_6O_{14}$
fw	1903.7
cell setting, space group	triclinic, $P\bar{1}$
a, b, c (Å)	10.2959(2), 10.4928(2), 18.2320(3)
α, β, γ (deg)	93.4481(6), 94.2305(6), 102.2943(7)
V (Å^3)	1913.42(6)
Z	1
density (Mg/m^3)	1.651
radiation type	Mo Kα
θ range (deg)	4.09−25.01
F(000)	945
μ (mm^{-1})	0.792
crystal color	dark-green prism
data collection method	$\omega-2\theta$ scans
collected/unique reflns	19 394/10 598
criterion for obsd reflns	$I > 2\sigma(I)$
R_{int}	0.0870
range of h, k, l	$-12 < h < 12$ $-12 < k < 12$ $-21 < l < 21$
reflns/restraints/param	6695/0/529
GOF on F^2	1.055
R1, wR2 [$I > 2\sigma(I)$, 5370 reflns]	0.0785, 0.2177
R1, wR2 (all)	0.0940, 0.2334
temperature (K)	299

Discussion

Crystallography. The ladder structure of **2** incorporates antiparallel Co···Pyrim−Ph−NO−Co···Pyrim−Ph−NO chains cross-linked by $Co(hfac)_2$ units at the pyrimidine units. The 4NITPhPyrim units are somewhat twisted, with phenyl−nitroxide and phenyl−pyrimidine dihedral angles of 34.1° and 21.6°. Both Co^{II} ions coordinate in pseudo-octahedral environments. The cross-linking Co^{II} coordinates axially to pyrimidine (for the longest bonds, see Table 2), with all hfac Co−O bonds equatorial. In the chains, the shortest Co−O bond is Co1−O1N1 at 2.022 Å: it is trans to the longest bond, Co1−O3 at 2.081 Å. The short Co1−O1 bond length is consistent with AFM spin pairing between the unpaired electrons in the Co^{II} and nitroxide. The Co−ON bond lengths in the related complexes **4**[5] and **5**[6] (Chart 2) are short at 2.06 and 2.09 Å, respectively; these are consistent with their strongly AFM Co−ON coupling. The NO−Co−N(pyrim)

(5) Baskett, M.; Lahti, P. M.; Paduan-Filho, A.; Oliveira, N., Jr. *Inorg. Chem.* **2005**, 44 6725.
(6) Field, L. M.; Lahti, P. M. *Inorg. Chem.* **2003**, *42*, 7447.

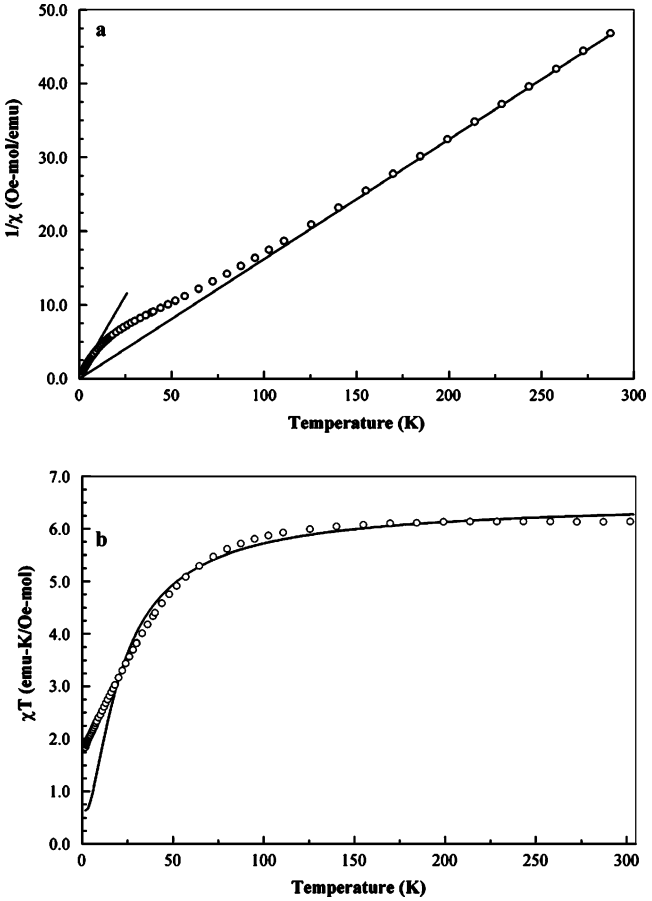

Figure 2. $1/\chi$ vs T (a) and χT vs T (b) plots for **2** obtained at 100 Oe. The solid lines in part a show Curie−Weiss fits for $1/\chi(T > 100$ K) and for $1/\chi(T < 7$ K). Part b shows a solid-line, nonlinear least-squares fit to $\chi T(T > 18$ K) data (circles) for eq 2, extrapolated to 2 K.

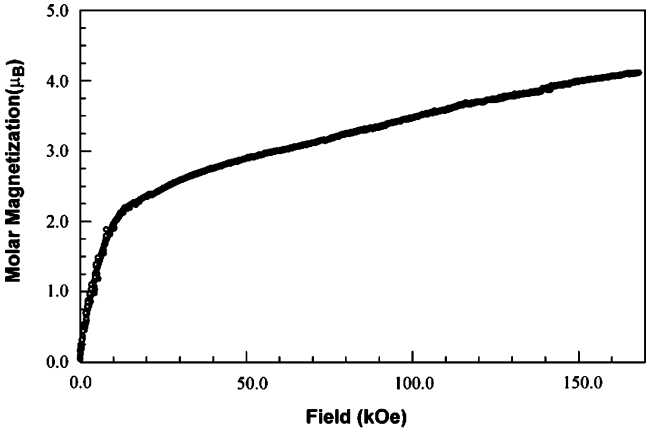

Figure 3. Molar magnetization versus field plot for **2** obtained at 1.35 K.

angle is 89°, similar to that seen for the analogous unit in dimers **1**, **4**, and **5**. The $[Co^{II}RL]_n$ chains in **2** are neither linear nor helical but are "step" ladders, with all nitroxide groups syn along the chain.

Magnetism. The $1/\chi$ vs T data for **2** over $T > 100$ K yield a high-temperature Curie constant of $C = 6.27$ emu·K/Oe·mol and a Weiss constant of $\theta = (-)5.5$ K (Figure 2a). The Curie constant shows strongly AFM coupling in the Co−ON linkages with $S_{Co-ON} = 1$. Using eq 1 with one average Landé constant for all spin carriers [$g_{Co} = g_{Co-ON} = g_{avg}$]

Table 2. Selected Bonding Parameters for Complex **2**

cross-link		1-D chain	
r(Co2−O7)	2.041(4)	r(N1−O1)	1.291(5)[a]
r(Co2−O6)	2.056(3)	r(Co1−O1N)	2.022(4)[a]
r(Co2−N1)	2.157(4)	r(Co1−O2)	2.033(4)
		r(Co1−O3)	2.081(5)
		r(Co1−O4)	2.029(4)
		r(Co1−N3)	2.159(4)
∠(N2−Co2−O6)	93.61(15)	∠(N1−O1−Co1)	122.9(3)[a]
∠(N2−Co2−O7)	90.97(16)	∠(O1−Co1−N3′)	88.96(16)[a]
∠(N2−Co2−N2′)	180.0	∠(O1−Co1−O3)	174.25(16)[a]
∠(O6−Co2−O7)	88.71(15)	∠(O1−Co1−O2)	90.49(17)[a]
∠(O6−Co2−O7′)	91.29(15)	∠(O1−Co1−O4)	95.90(16)[a]
∠(O6−Co2−O6′)	180.0	∠(O1−Co1−O5)	95.45(15)[a]
∠(O7−Co2−O7′)	180.0	∠(O5−Co1−N3′)	175.56(17)
		∠(O3−Co1−N3′)	86.01(18)

[a] Involves nitroxide N1O1. All bond lengths are in angstroms and bond angles in degrees; estimated standard deviations are in parentheses. See Figure 1 for all numbering schemes.

Chart 2

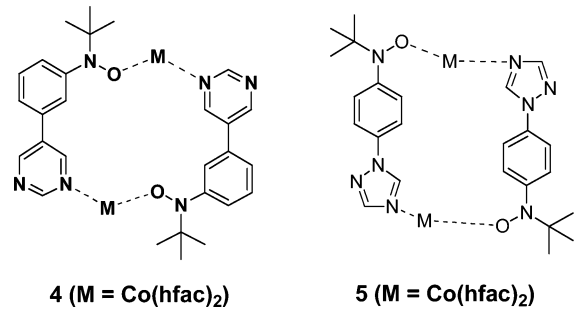

yields $g_{avg} = 2.54$. If we assume that $g_{Co-ON} = 2.45$ by comparison to values obtained[5] for dimer complex **4** (a fairly close structural model for the Co−ON units in **2**), then eq 1 yields $g_{Co} = 2.64$. This is a reasonable value for octahedral high-spin Co^{II} complexes.[7]

$$C = \frac{N\beta^2}{3k}[2g_{Co-ON}{}^2 S_{Co-ON}(S_{Co-ON}+1) + g_{Co}{}^2 S_{Co}(S_{Co}+1)] \quad (1)$$

Below about 70 K, the $\chi T(T)$ data (Figure 2b) decrease strongly toward an ordinate intercept of ∼2 emu·K/Oe·mol. A Curie plot of $1/\chi$ vs T for $T < 7$ K yields $C \sim 2.44$ emu·K/Oe·mol (Figure 2a). In the low-temperature regime, octahedral Co^{II} typically acts as a low-spin species.[7] Given the strongly AFM exchange in the Co1−O1N units, if $S_{Co1-O1N} = 0$ when the temperature drops below about 10 K, then only the $Co(hfac)_2$ cross-links (Co2) contribute significantly to the overall magnetic susceptibility. Applying eq 1 to the Curie constant for $T < 7$ K with $S_{Co} = {}^1/_2$ and $S_{Co-ON} = 0$ yields $g_{Co} \sim 5.1$. A typical value[7] for octahedral low-spin Co^{II} ions is $g \sim 4.3$. Although **2** deviates strongly from Curie−Weiss behavior at low temperature, this crude estimate is consistent with expectations for a low-spin Co^{II} cross-linker ion.

The molar magnetization at 1.35 K (Figure 3) rises rapidly to ∼2.2−2.5 μ_B at 15−20 kOe; at higher fields, there is a gradual rise up to the maximum measured field of 170 kOe.

(7) Compare: Carlin, R. L. *Magnetochemistry*; Springer-Verlag: Berlin, Germany, 1986; pp 65 and 66.

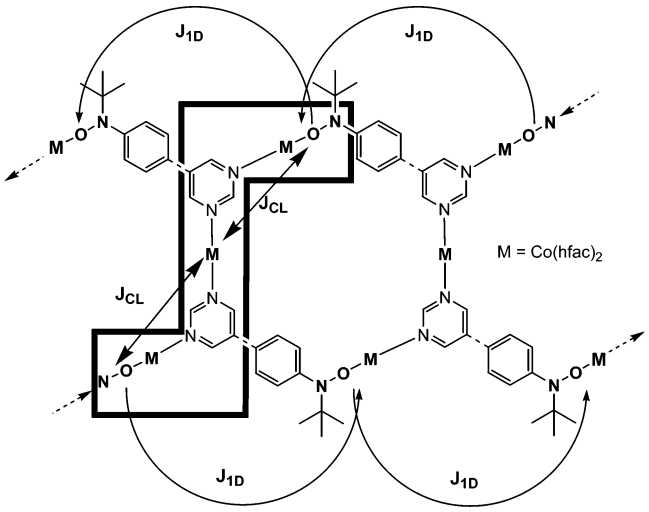

Figure 4. Schematic representation correlating proposed exchange interactions with structural features in **2**.

These data appear to combine contributions to M vs H behavior that are similar to behaviors seen in the $Co(RL)_2(hfac)_2$ complex[4] **3** and the $Co_2(RL)_2(hfac)_4$ dimer[5] **4**. This is not surprising if one considers the spin units in **2** to be weakly coupled because systems **3** and **4** separately have structural features that are combined in **2** itself. M_{molar} vs H for **3** rises rapidly up to M_{molar}(15−20 kOe) ∼ 2.0−2.2 μ_B and then saturates at roughly 3 μ_B.[4] M_{molar} vs H for **4** rises throughout 0−170 kOe at 1.4 K.[5] Similarly, M_{molar} vs H for related complex **5** increases nearly linearly at 1.8 K up to the maximum field of 50 kOe used in that study.[6] We assign the lower-field, rapid-rise regions of M_{molar} vs H for **2** (and **3**) to the pyrimidine-coordinated Co^{II} units in each. Unlike the case in **3**, the magnetization of **2** does not saturate after the initial rise because of the higher-field, rising M vs H contributions from its Co−ON units, analogously to the behaviors of **4** and **5**, which also contain Co−ON units. Although one magnetic orbital in the Co−ON units is spin-paired with the nitroxide singly occupied molecular orbital (SOMO), there remain two magnetic orbitals that can give rise to singlet and triplet states. As the field increases, the paramagnetic state of Co−ON apparently becomes populated, leading to the increase in measured magnetization.

Magnetically, **2** can be considered a ladder (Figure 4) where J_{1D} is intrachain (rail) exchange and J_{CL} cross-linking (rung) exchange. Because of the complexity of the system, a full analysis of all plausible exchange interactions was not carried out. However, assuming $J_{1D} \ll J_{CL}$, the ladder reduces to a linear three-spin-unit model with two $S = 1$ Co−ON units coupled through a central $S = {}^3/_2$ Co^{II} unit. This model was chosen because it seemed unlikely that the J_{1D} exchange interactions along the −Co−RL−Co−RL− chains would be strongly propagated across the bond that links the pyrimidine to the phenyl nitroxide unit in the RL = 4NITPhPyrim ligands. Although 4NITPhPyrim is conjugated and can, in principle, accommodate spin-polarized exchange across both rings in its structure, solution electron spin resonance and computational studies have shown[2] that little nitroxide spin density delocalizes onto the pyrimidine unit of the isolated radical.

Equation 2 was used to fit the magnetic behavior of **2** by the three-spin-unit model, using an averaged Landé factor g_{avg} and $J/k = J_{CL}$ (Figure 4).[8] J_{CL} here is an effective exchange constant that can include contributions from the Co^{II} paramagnetic, temperature-dependent, spin-state population variations and zero-field-splitting effects, especially at lower temperatures.

$$\chi T = (N\beta^2 g_{avg}{}^2/3k)\{[126e^{6J/kT} + 52.5(e^{-J/kT} + e^{3J/kT}) + 15(e^{-6J/kT} + e^{-2J/kT} + 1) + 1.5(e^{-9J/kT} + e^{-5J/kT})]/[8e^{6J/kT} + 6(e^{-J/kT} + e^{3J/kT}) + 4(e^{-6J/kT} + e^{-2J/kT} + 1) + 2(e^{-9J/kT} + e^{-5J/kT})]\} \quad (2)$$

This model did not fit the data well for the full temperature range, which is not surprising because of the electronic complexities of the system. Figure 2b shows the model curve fitted to the data where $T > 18$ K (but extrapolating the curve down to 2 K). The fit yielded $g_{avg} = 2.61 \pm 0.06$ and $J_{CL} = (-)5.3 \pm 0.9$ K $= (-)3.7 \pm 0.6$ cm^{-1} (uncertainties are 1 standard deviation). Fitting of the data in the same manner for $T > 40$ K yielded $g_{avg} = 2.65 \pm 0.05$ and $J_{CL} = (-)5.9 \pm 0.5$ K $= (-)4.1 \pm 0.4$ cm^{-1}, so effects of the spin-state population variation in Co^{II} do not much change the estimate of J_{CL} at these temperatures. Inclusion of a mean-field Weiss term ($T - \theta$) did not improve the fit significantly.

Scheme 1 applies to **2** the same π-spin polarization paradigms as those used to explain[2] AFM exchange in **1**. The chain (rail) portions of **2** should contribute AFM exchange ($J_{1D} < 0$; Scheme 1A), so if J_{1D} is significant, this should contribute to the overall AFM χT downturn in **2**. However, if J_{CL} dominates, its AFM nature deserves explanation, especially because *m*-arylene units are commonly considered[9] to be archetypical FM exchange linkage groups, albeit with some known violations.[10] A π-spin polarization model for pyrimidine predicts FM RLCo···Co^{II}···CoLR exchange ($J_{CL} > 0$; Scheme 1B). However, although pyrimidine is a FM exchange linker in some cases,[11] it also is known to behave as an AFM exchange linker.[12] For example, Ishida et al.[12c] recently showed that dinuclear M−L−M complexes **6** (Chart 3) all have AFM exchange coupling between the inorganic ions. The following discussion is based on this work and show how the three-spin-unit

(8) Mabbs, F. E., Machin, D. J., Eds. *Magnetism and Transition Metal Complexes*; Wiley: New York, 1973; Chapter 7.
(9) (a) Borden, W. T., Ed. *Diradicals*; John Wiley and Sons: New York, 1982. (b) Berson, J. A. In *The Chemistry of Quinoid Compounds*; Patai, S., Rappaport, Z., Eds.; John Wiley and Sons: New York, 1988; Vol. 2, pp 462−469.
(10) Borden, W. T.; Iwamura, H.; Berson, J. A. *Acc. Chem. Res.* **1994**, *27*, 109.
(11) (a) Mitsubori, S.; Ishida, T.; Nogami, T.; Iwamura, H. *Chem. Lett.* **1994**, 285. (b) Mitsubori, S.; Ishida, T.; Nogami, T.; Iwamura, H.; Takeda, N.; Ishikawa, M. *Chem. Lett.* **1994**, 685. (c) Ishida, T.; Mitsubori, S.; Nogami, T.; Ishikawa, Y.; Yasui, M.; Iwasaki, F.; Iwamura, H.; Takeda, N.; Ishikawa, M. *Synth. Met.* **1995**, *71*, 1791.
(12) (a) Ishida, T.; Mitsubori, S.; Nogami, T.; Iwamura, H. *Mol. Cryst. Liq. Cryst. Sci. Technol., Sect. A* **1993**, *233*, 345. (b) Munno, G. D.; Poerio, T.; Julve, M.; Lloret, F.; Viau, G. *New J. Chem.* **1998**, *22*, 299. (c) Ishida, T.; Kawakami, T.; Mitsubori, S.; Nogami, T.; Yamaguchi, K.; Iwamura, H. *J. Chem. Soc., Dalton Trans.* **2002**, 3177.

Scheme 1. Possible Qualitative Exchange Mechanisms in **2**

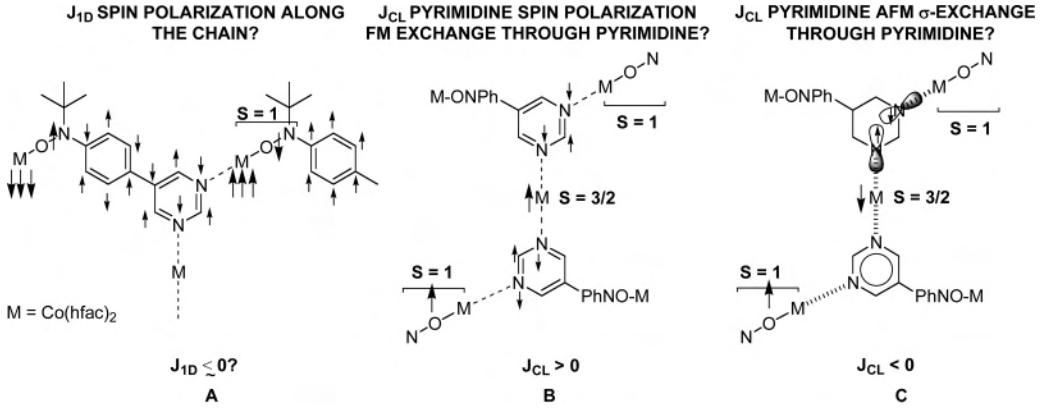

approximation of eq 2 with $J_{1D} \ll J_{CL}$ can qualitatively account for the observed AFM exchange behavior of **2**.

Computations indicate that pyrimidine can provide a σ-type or superexchange mechanism that outweighs π-spin polarization effects (Scheme 1C).[12c,13] When paramagnetic ions polarize the pyrimidine nitrogen spin densities, a cross-ring nσ overlap gives AFM exchange between the ions. This confounds simple π-connectivity-based comparisons with the all-carbon FM coupling *m*-phenylene unit.

The qualitative exchange behavior of pyrimidine depends on the strength of its interaction with the magnetic orbitals of a metal ion. For example, Glaser et al. have argued[14] that the AFM exchange between Cu^{II} ions in dinuclear complex $\{CuCl_2\}(tptz)\{CuCl_2 \cdot (MeOH)\}$ (**7**) comes from a π-spin polarization pathway involving the triazinyl ring and an attached pyridine ring due to the very weak direct exchange pathway through a long $Cu^{II}-N$(triazine) bond, shown as a dashed line in **7**. However, M−L−M exchange in variants of **6** supports[12c,13] the following typical generalizations: (1) when there is good dσ−nσ orbital overlap at both nitrogens of pyrimidine, AFM exchange coupling is favored; (2) high-spin Co^{II} ions will be AFM coupled by pyrimidine regardless of whether they are coordinated axial−axial, axial−equatorial, or equatorial−equatorial because high-spin Co^{II} has both axial and equatorial (d_{z^2} and $d_{x^2-y^2}$) magnetic orbitals available to participate in AFM-favoring dσ−nσ metal−pyrimidine overlap.

Figure 5 summarizes the proposed exchange interactions in **2**. Within the Co−ON units, one magnetic orbital overlaps strongly with the nitroxide SOMO to give AFM exchange regardless of axial or equatorial coordination, giving the observed higher temperature $S = 1$ state ($J_{Co-ON} \ll 0$, shown as a solid-line bond). In the same Co−ON unit, another Co magnetic orbital overlaps with a pyrimidine nσ orbital. J_{CL} between a Co−ON and Co cross-link occurs through this dσ−nσ overlap, $J_{CL} \ll 0$. Across the Pyrim−PhNIT bond in the RL, J_{1D} is assumed to be quite small (dotted bond) by analogy to the behavior observed[2] in complexes **1** and so is not shown in detail.

Lower-dimensional molecular coordination complexes can exhibit slow magnetic relaxation with unique magnetic properties in 0-D clusters.[14,15] Some 1-D systems can also exhibit slow relaxation, as described by Glauber[16] and demonstrated by Caneschi et al. in a paper describing[17] the hysteresis behavior of a 1:1, 1-D helical chain complex of $Co(hfac)_2$ with 2-(4-methoxyphenyl)-4,4,5,5-tetramethylimidazoline-1-oxyl 3-oxide. However, ac susceptibility measurements on **2**, collected between 1.8 and 4.2 K, showed χ'' to be only about 1% of χ', so no further such studies were attempted.

Overall, it does not appear that **2** acts as a ferromagnet chain, despite the possibilities presented by having two different spin units. Of course, the overall behavior of **2** at low temperature is much influenced by the fact that the strongly AFM exchange coupled Co^{II}RL units contribute no net magnetic moment to the system at lowest temperatures, leading to a situation where the Co^{II} cross-linkers are the only significant magnetic moment contributors.

Conclusions

The complexation of 4NITPhPyrim (RL) with $Co(hfac)_2$ yields a 1-D structural ladder polymer complex **2** with stoichiometry $Co_3(RL)_2(hfac)_6$ rather than a $M_2(RL)_2(hfac)_4$ cyclic dimer, as found for reactions with $Mn(hfac)_2$ and $Cu(hfac)_2$. The complex has a very strong AFM exchange within $Co^{II}-ON$ bonds that make these net $S = 1$ units.

Chart 3

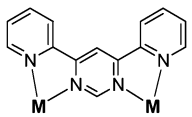

6 (M = $Mn(hfac)_2$, $Co(hfac)_2$, $Ni(hfac)_2$, $Cu(hfac)_2$

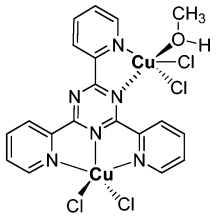

7

(13) Mohri, F.; Yoshizawa, K.; Yamabe, T.; Ishida, T.; Nogami, T. *Mol. Eng.* **1999**, *8*, 357.
(14) Glaser, T.; Lügger, T.; Fröhlich, R. *Eur. J. Inorg. Chem.* **2004**, 394.
(15) (a) Sessoli, R.; Gatteschi, D.; Caneschi, A.; Novak, M. A. *Nature* **1993**, *365*, 141. (b) Gatteschi, D.; Caneschi, A.; Pardi, L.; Sessoli, R. *Science* **1994**, *265*, 1054. (c) Friedman, J. R.; Sarachik, M. P.; Tejada, J.; Ziolo, R. *Phys. Rev. Lett.* **1996**, *76*, 3830.
(16) Glauber, R. J. *J. Math. Phys.* **1963**, *4*, 294.
(17) Caneschi, A.; Gatteschi, D.; Lalioti, N.; Sangregorio, C.; Sessoli, R.; Venturi, G.; Vindigni, A.; Rettori, A.; Pini, M. G.; Novak, M. A. *Angew. Chem., Int. Ed.* **2001**, *40*, 1760.

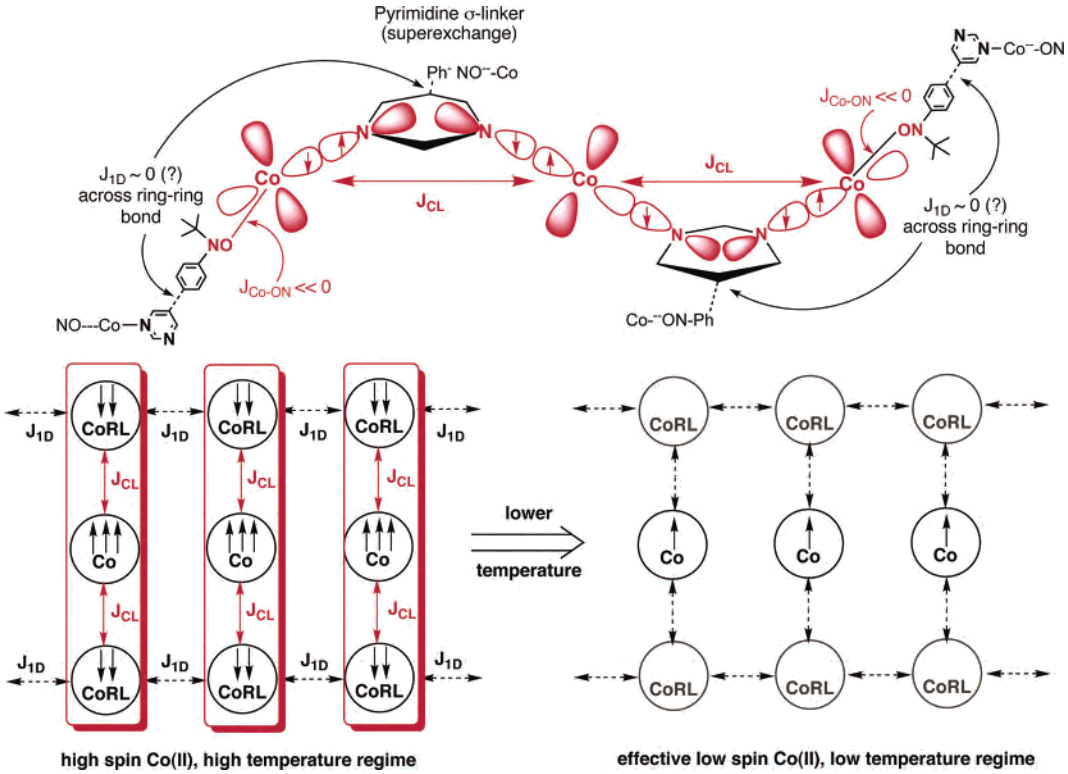

Figure 5. Orbital basis of exchange interactions proposed in **2** with the three-spin-unit model of eq 2 shown in red in the upper chart. The lower chart shows a spin-array schematic for high- and low-temperature regimes.

Superexchange or σ-type mechanisms through pyrimidine qualitatively explain the overall AFM exchange through the cross-links between Co^{II} and Co−ON units. The complex shows no evidence of ferrimagnetic behavior despite having subunits with different effective spin quantum numbers that are nominally linked through the conjugated organic radical ligands. Although it is difficult to prove definitively, it seems likely that exchange throughout the structural network of **2** is significantly reduced by poor coupling through the chains (J_{1D}), across the intramolecular bond linking the pyrimidine and phenyl groups of 4NITPhPyrim units. The overall magnetic behavior is influenced more by direct metal−ligand exchange couplings than by extended coupling through the nominally conjugated network.

Experimental Section

5-[4-(*N*-*tert*-Butyl-*N*-aminoxyl)phenyl]pyridimine (4NITPh-Pyrim). This radical was made by a previously described[2] literature method.

Co_3(4NITPhPyrim)$_2$(hfac)$_6$ (2). A solution of 0.160 g (0.34 mmol) of Co(hfac)$_2$·xH$_2$O in 4 mL of 1:1 (v:v) dichloromethane/hexane was carefully layered on top of 0.053 g (0.22 mmol) of radical 4NITPhPyrim in 2 mL of dichloromethane; then 2 mL of hexane was layered atop the mixture. The resulting mixture was allowed to stand and evaporate slowly to yield 0.125 g (58%) of dark-green crystals, mp 222−224 °C (dec). Anal. Calcd for $C_{58}H_{38}N_6O_{14}F_{36}Co_3$: C, 36.60; H, 2.01; N, 4.42. Found: C, 37.46; H, 2.08; N, 4.41. Crystal data: $C_{58}H_{38}F_{36}Co_3N_6O_{14}$, $M = 1903.697$, triclinic, $P\bar{1}$, $a = 10.2959(2)$ Å, $b = 10.4928(2)$ Å, $c = 18.2320(3)$ Å, $\alpha = 93.4481(6)°$, $\beta = 94.2305(6)°$, $\gamma = 102.2943(7)°$, $V = 1913.42(6)$ Å^3, $Z = 1$, $\mu = 0.792$ mm^{-1}, $T = 293$ K, data/parameters = 6695/529, converging to R1 = 0.0785, wR2 = 0.2177 (on 5370 observed data with $I > 2\sigma(I)$); R1 = 0.0940, wR2 = 0.2334. ORTEP diagrams were generated using ORTEP-III.[18] Additional information was deposited with the Cambridge Crystallographic Databank, CCDC Deposition No. 288149.

Magnetic susceptibility (χ) versus temperature measurements for **2** were carried out at 100 Oe over 1.8−300 K using a Quantum Design MPMS-5 SQUID magnetometer, using polycrystalline samples placed in gelatin capsules and held in place with a small amount of cotton; susceptibility data were corrected for temperature-independent paramagnetic contributions (χ_{TIP}) based on the high-temperature $\chi T(T)$ data. Magnetization versus field (M_{molar} vs H) studies were carried out on powdered samples at 1.35 K over 0−170 kOe using a custom-built vibrating sample magnetometer apparatus of a type that has been described[19] elsewhere.

Acknowledgment. This material is based upon work supported by the National Science Foundation by Grants CHE-0109094 and CHE-0415716, the Comision Interministerial de Ciencia y Tecnologia (CICYT-MAT2004-03395-C02-01), the Fullbright España, and the Fundação de Amparo a Pesquisado Estado de São Paulo. Support for the University of Massachusetts Amherst X-ray Structural Characterization Facility (NSF Grant CHE-9974648) and Nanomagnetics Characterization Facility (NSF Grant CTS-0116498) was provided by the National Science Foundation. We thank Dr. A. Chandrasekaran for crystallographic analyses.

Supporting Information Available: Crystallographic data for **2** in CIF format. This material is available free of charge via the Internet at http://pubs.acs.org.

IC051884W

(18) Farrugia, L. J. *J. Appl. Crystallogr.* **1997**, *30*, 565.
(19) Oliveira, N. F., Jr.; Foner, S. *Rev. Sci. Instrum.* **1972**, *43*, 37.